Electronic Supplementary Material (ESI) for Nanoscale.

Supplementary Information:
Vibronic effect and influence of aggregation on the photophysics of graphene quantum dots

Thomas Liu,[1] Claire Tonnelé,[2] Shen Zhao,[1] Loïc Rondin,[1] Christine Elias,[1] Daniel Medina-Lopez,[3] Hanako Okuno,[4] Akimitsu Narita,[5] Yannick Chassagneux,[6] Christophe Voisin,[6] Stéphane Campidelli,[3] David Beljonne,[2] and Jean-Sébastien Lauret[1]
[1]Université Paris-Saclay, ENS Paris-Saclay, CentraleSupélec, CNRS, LuMIn, Orsay, France
[2]CMN, Université MONS, Belgium
[3]Université Paris-Saclay, CEA, CNRS, NIMBE, LICSEN, 91191, Gif-sur-Yvette, France.
[4]University Grenoble Alpes, CEA INAC-MEM, F-38000 Grenoble, France
[5]Max Planck Institute for Polymer Research, Ackermannweg 10, 55128 Mainz, Germany
[6]LPENS, PSL, CNRS, Université de Paris, Sorbonne Université, 75005 Paris, France

E-mail: lauret@ens-paris-saclay.fr

Computational Results

Visualization of normal modes and input files for the analysis of the variations of excitation energies and oscillator strengths along normal mode deformation have been done using the DrawMol program [DrawMol, Vincent LIEGEOIS, UNamur, www.unamur.be/drawmol]. Other visualizations have been done using VMD [Humphrey, W.; Dalke, A.; Schulten, K. VMD: Visual Molecular Dynamics. J. Mol. Graphics 1996, 14, 33−38.]

Equilibrium geometry of $C_{96}C_{12}$ GQD monomer in gas phase

Two equilibrium geometries were obtained, exhibiting a non-planar core and differing essentially in the orientation of the alkyl chains with respect to the core of the nanographene, namely lying perpendicular (**a**) or planar (**b**) relative to the latter (Figure S1). With both M062-X and HSE06, **a** is computed to be the most stable conformer by 5.7 and 6.7 kcal.mol^{-1}, respectively. To evaluate the possible structural difference between the core of **a** and **b**, we computed the RMSD and obtained negligible values of 0.05 Å and 0.09 Å, respectively, indicating that the core is virtually unaffected by the orientation of the alkyl chains (central ring of both conformers aligned prior to RMSD calculation). In this work, we thus considered only conformer **a**.

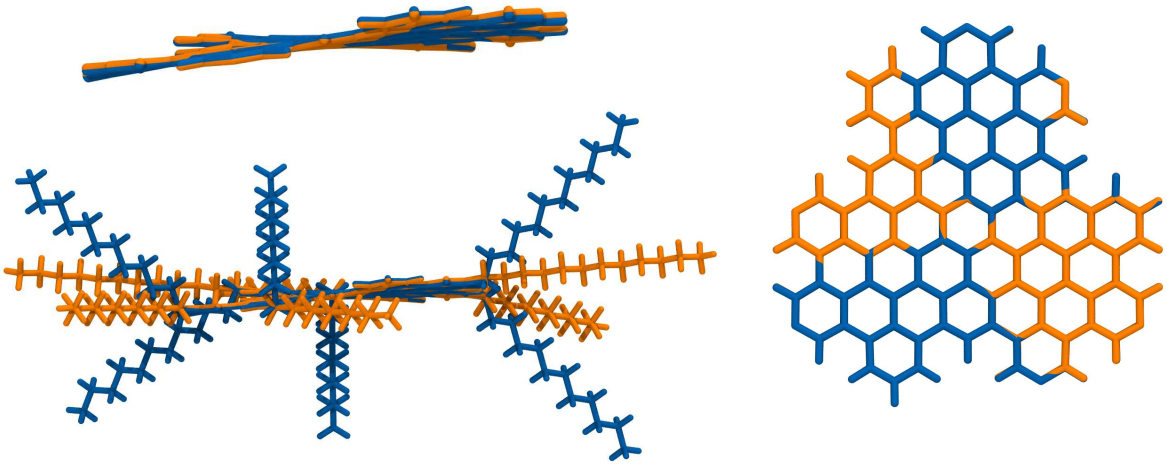

Figure S1. Equilibrium geometries of GQD conformers **a** (blue) and **b** (orange) computed at the M062-X/6-31g(d) level.

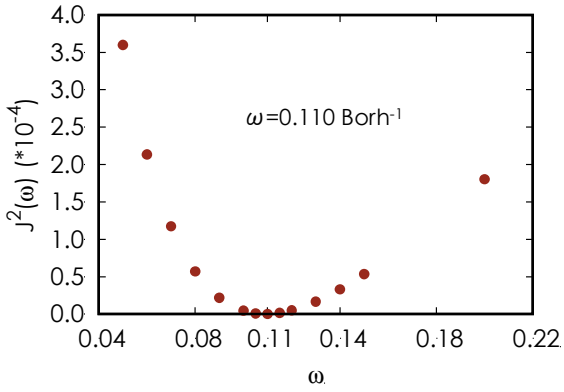

Figure S2. LC-wPBE tuning of w – on B3LYP/6-31G(d) optimized geometry.

Figure S2 illustrates the procedure for tuning the omega parameter of the functional. It is part of the "range-separated hybrid" family which allows a partition of the short-range / long-range Coulomb operator with an error function. The operator then depends on the omega parameter which can be optimized in a non-empirical way by minimizing the following term:

$$J^2(\omega) = \sum_{i=0}^{1} \left[\varepsilon_H(N+i) + IP^{\omega}(N+i) \right]^2$$

Table S1. Excitation energies (in eV) at the B3LYP/6-31G(d) level using geometries obtained with different energy functionals and the 6-31G(d) basis set in vacuum. Oscillator strengths indicated in parentheses.

Geometry	**B3LYP**	**HSE06**	**M062X**
S1	2.12 (0.00)	2.13 (0.00)	2.18 (0.00)
S2	2.20 (0.00)	2.21 (0.00)	2.26 (0.00)
S3	2.57 (1.57)	2.58 (1.56)	2.62 (1.55)
S4	2.57 (1.57)	2.58 (1.57)	2.62 (1.56)

Table S2. Excitation energies (in eV) obtained with different energy functionals and the 6-31G(d) basis set in vacuum using the B3LYP/6-31G(d) geometry. Oscillator strengths indicated in parentheses.

TD	**B3LYP**	**HSE06**	**M062X**	**wB97XD**	**LC-wPBE**
S1	2.12 (0.00)	2.12 (0.00)	2.50 (0.00)	2.57 (0.00)	2.13 (0.00)
S2	2.20 (0.00)	2.20 (0.00)	2.66 (0.00)	2.73 (0.00)	2.25 (0.00)
S3	2.57 (1.57)	2.54 (1.49)	3.10 (2.59)	3.29 (2.98)	2.64 (1.79)
S4	2.57 (1.57)	2.55 (1.49)	3.10 (2.59)	3.29 (2.99)	2.64 (1.79)

Table S3. Excitation energies (eV), wavelength (nm), oscillator strength (*f*) and dominant contributions (%) computed with LC-ωPBE XCF on the basis of B3LYP geometry.

LC-ωPBE	TDDFT			main
state	ΔE	λ	*f*	contributions (TD)
S_1	2.130	582	0.000	47 H-1 → L 47 H → L+1
S_2	2.251	551	0.000	47 H-1 → L+1 48 H → L
S_3	2.644	469	1.792	44 H-1 → L 44 H → L+1
S_4	2.644	469	1.791	45 H-1 → L+1 44 H → L

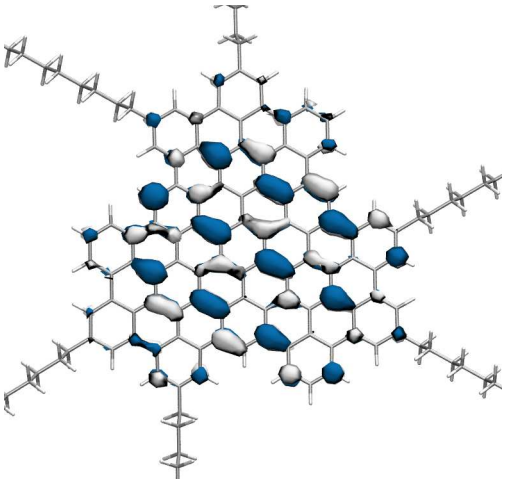

LUMO (-1.353 eV)

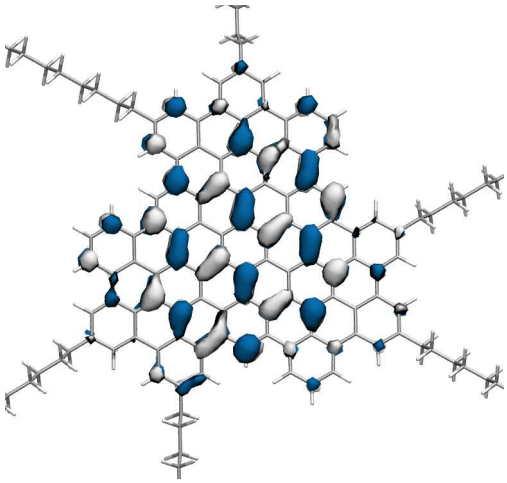

LUMO+1 (-1.350 eV)

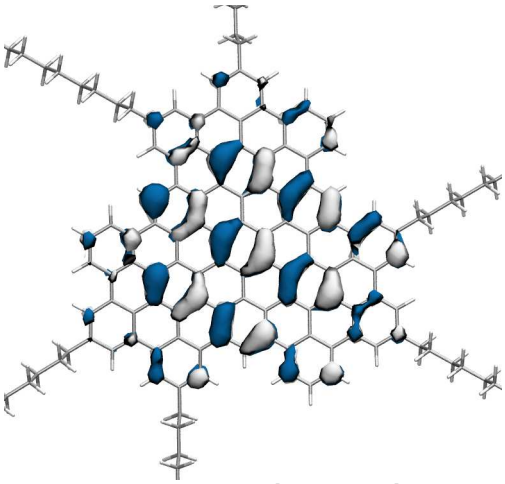

HOMO (-5.567 eV)

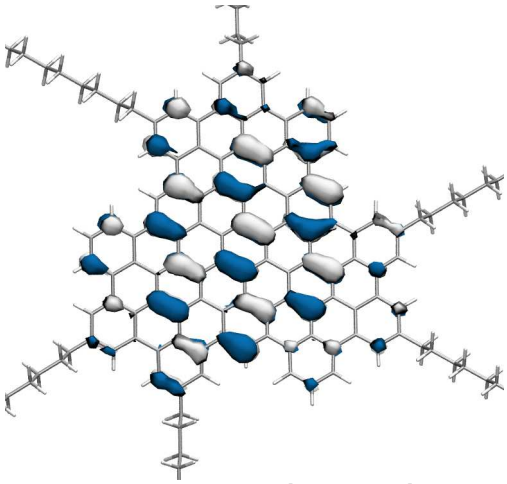

HOMO-1 (-5.570 eV)

Figure S3. Frontier molecular orbitals of $C_{96}C_{12}$ GQD.

Table S4. Excitation energies (eV) and oscillator strength (in parentheses) computed with LC-ωPBE XCF for monomer geometries extracted from the MD simulation.

frame	S1	S2	S3	S4	S5	S6
b900	2.06 (0.00)	2.17 (0.06)	2.56 (1.53)	2.58 (1.48)	3.82 (2.67)	2.69 (0.06)
b925	2.03 (0.01)	2.15 (0.03)	2.55 (1.63)	2.56 (1.44)	3.67 (2.61)	2.67 (0.00)
b950	2.02 (0.00)	2.14 (0.02)	2.54 (1.65)	2.55 (1.59)	4.07 (2.60)	2.66 (0.11)
b975	2.03 (0.00)	2.12 (0.16)	2.55 (1.62)	2.60 (1.53)	3.98 (2.64)	2.68 (0.01)
c000	1.99 (0.00)	2.12 (0.01)	2.51 (1.60)	2.52 (1.55)	3.91 (2.59)	2.63 (0.09)
c025	2.04 (0.01)	2.16 (0.03)	2.56 (1.70)	2.57 (1.61)	4.14 (2.63)	2.68 (0.03)
c050	2.00 (0.00)	2.12 (0.05)	2.51 (1.60)	2.54 (1.56)	3.96 (2.61)	2.66 (0.02)
c075	1.97 (0.00)	2.10 (0.02)	2.50 (1.63)	2.51 (1.62)	4.07 (2.61)	2.64 (0.02)
c100	2.05 (0.00)	2.17 (0.03)	2.56 (1.64)	2.57 (1.60)	4.12 (2.64)	2.67 (0.02)
c125	2.03 (0.00)	2.14 (0.05)	2.55 (1.60)	2.56 (1.58)	4.05 (2.65)	2.66 (0.01)
c150	2.07 (0.00)	2.19 (0.05)	2.59 (1.54)	2.59 (1.60)	4.15 (2.64)	2.71 (0.02)
c175	1.99 (0.00)	2.11 (0.03)	2.52 (1.70)	2.53 (1.63)	4.13 (2.66)	2.68 (0.01)
c200	2.07 (0.01)	2.14 (0.19)	2.57 (1.48)	2.62 (1.13)	2.96 (2.64)	2.71 (0.05)
c225	2.05 (0.00)	2.17 (0.05)	2.58 (1.68)	2.59 (1.68)	4.34 (2.64)	2.68 (0.00)
c250	2.06 (0.00)	2.19 (0.01)	2.58 (1.68)	2.59 (1.59)	4.10 (2.66)	2.69 (0.08)
c275	1.99 (0.00)	2.11 (0.05)	2.52 (1.65)	2.54 (1.63)	4.14 (2.61)	2.64 (0.02)
c300	2.08 (0.00)	2.20 (0.01)	2.59 (1.62)	2.60 (1.65)	4.28 (2.66)	2.70 (0.02)
c325	2.05 (0.00)	2.15 (0.14)	2.57 (1.59)	2.60 (1.42)	3.70 (2.65)	2.70 (0.01)
c350	2.02 (0.00)	2.14 (0.01)	2.54 (1.71)	2.55 (1.67)	4.25 (2.61)	2.64 (0.00)
c375	2.06 (0.00)	2.17 (0.09)	2.58 (1.64)	2.60 (1.44)	3.73 (2.63)	2.70 (0.00)
c400	2.02 (0.00)	2.13 (0.05)	2.54 (1.72)	2.56 (1.60)	4.09 (2.63)	2.67 (0.01)
c425	1.99 (0.00)	2.11 (0.00)	2.51 (1.53)	2.52 (1.64)	4.14 (2.60)	2.65 (0.09)
c450	2.03 (0.00)	2.15 (0.05)	2.55 (1.60)	2.55 (1.64)	4.18 (2.61)	2.63 (0.00)
c475	2.03 (0.00)	2.14 (0.06)	2.55 (1.70)	2.56 (1.41)	3.60 (2.61)	2.65 (0.02)
c500	2.04 (0.00)	2.15 (0.08)	2.56 (1.68)	2.57 (1.61)	4.14 (2.61)	2.67 (0.00)
c525	2.02 (0.00)	2.14 (0.00)	2.54 (1.72)	2.55 (1.69)	4.31 (2.62)	2.66 (0.04)
c550	2.06 (0.00)	2.16 (0.08)	2.58 (1.75)	2.59 (1.49)	3.86 (2.65)	2.67 (0.00)
c575	1.99 (0.01)	2.11 (0.01)	2.51 (1.68)	2.52 (1.52)	3.84 (2.61)	2.63 (0.08)
c600	2.02 (0.00)	2.14 (0.01)	2.54 (1.65)	2.55 (1.65)	4.20 (2.63)	2.68 (0.03)
c625	2.05 (0.00)	2.18 (0.00)	2.56 (1.69)	2.57 (1.60)	4.11 (2.61)	2.68 (0.04)
c650	2.02 (0.00)	2.14 (0.02)	2.53 (1.50)	2.55 (1.63)	4.17 (2.62)	2.64 (0.16)
c675	2.01 (0.00)	2.12 (0.13)	2.53 (1.53)	2.57 (1.53)	3.94 (2.60)	2.63 (0.04)
c700	2.00 (0.00)	2.13 (0.00)	2.51 (1.59)	2.53 (1.67)	4.23 (2.62)	2.65 (0.02)
c725	2.01 (0.01)	2.13 (0.05)	2.53 (1.58)	2.55 (1.57)	4.00 (2.59)	2.65 (0.13)
c750	2.03 (0.00)	2.14 (0.08)	2.54 (1.68)	2.57 (1.46)	3.75 (2.62)	2.64 (0.01)
c800	2.03 (0.00)	2.14 (0.05)	2.55 (1.62)	2.56 (1.62)	4.15 (2.62)	2.68 (0.01)
c825	2.04 (0.01)	2.17 (0.01)	2.56 (1.65)	2.57 (1.71)	4.40 (2.64)	2.66 (0.01)
c850	1.95 (0.00)	2.08 (0.01)	2.49 (1.74)	2.50 (1.64)	4.08 (2.57)	2.62 (0.02)
c875	2.03 (0.01)	2.15 (0.06)	2.55 (1.61)	2.56 (1.66)	4.26 (2.63)	2.67 (0.00)
c900	2.04 (0.00)	2.15 (0.05)	2.55 (1.56)	2.58 (1.62)	4.17 (2.61)	2.67 (0.01)
c925	2.01 (0.00)	2.13 (0.02)	2.54 (1.70)	2.55 (1.66)	4.23 (2.66)	2.67 (0.01)
c950	2.00 (0.01)	2.14 (0.00)	2.53 (1.59)	2.54 (1.63)	4.14 (2.62)	2.63 (0.02)
c975	2.00 (0.00)	2.11 (0.06)	2.52 (1.64)	2.55 (1.58)	4.02 (2.61)	2.67 (0.01)

Table S5. Excitation energies (eV) and oscillator strength (in parentheses) computed with LC-ωPBE XCF for dimer geometries extracted from the MD simulation.

Transition / frame number	h241	h415	h440	h656	h737	h878	h897
S1	1.99 (0.00)	1.88 (0.00)	1.92 (0.00)	1.97 (0.00)	2.00 (0.00)	1.92 (0.00)	1.96 (0.00)
S2	2.04 (0.00)	1.93 (0.00)	1.98 (0.00)	2.00 (0.00)	2.03 (0.00)	1.96 (0.00)	2.02 (0.00)
S3	2.10 (0.00)	1.97 (0.00)	2.02 (0.01)	2.08 (0.02)	2.09 (0.00)	2.04 (0.00)	2.05 (0.01)
S4	2.14 (0.00)	2.03 (0.01)	2.08 (0.00)	2.08 (0.02)	2.13 (0.01)	2.06 (0.00)	2.11 (0.00)
S5	2.17 (0.00)	2.05 (0.01)	2.09 (0.01)	2.14 (0.00)	2.19 (0.00)	2.13 (0.00)	2.16 (0.00)
S6	2.19 (0.00)	2.08 (0.00)	2.12 (0.00)	2.15 (0.00)	2.21 (0.00)	2.13 (0.01)	2.17 (0.00)
S7	2.22 (0.00)	2.09 (0.00)	2.15 (0.01)	2.19 (0.02)	2.21 (0.00)	2.15 (0.00)	2.18 (0.00)
S8	2.24 (0.00)	2.13 (0.00)	2.17 (0.00)	2.21 (0.00)	2.22 (0.00)	2.16 (0.00)	2.21 (0.00)
S9	2.25 (0.01)	2.17 (0.00)	2.18 (0.00)	2.23 (0.01)	2.25 (0.02)	2.18 (0.00)	2.23 (0.00)
S10	2.26 (0.02)	2.18 (0.01)	2.21 (0.01)	2.25 (0.00)	2.25 (0.00)	2.20 (0.00)	2.23 (0.00)
S11	2.28 (0.00)	2.21 (0.00)	2.25 (0.00)	2.26 (0.00)	2.27 (0.01)	2.21 (0.00)	2.26 (0.00)
S12	2.29 (0.00)	2.25 (0.00)	2.26 (0.01)	2.30 (0.01)	2.28 (0.00)	2.23 (0.00)	2.27 (0.00)
S13	2.39 (0.02)	2.35 (0.01)	2.37 (0.01)	2.37 (0.01)	2.38 (0.01)	2.34 (0.01)	2.38 (0.01)
S14	2.40 (0.01)	2.38 (0.01)	2.38 (0.00)	2.38 (0.02)	2.39 (0.02)	2.36 (0.01)	2.38 (0.03)
S15	2.53 (0.02)	2.48 (0.11)	2.45 (0.02)	2.52 (0.42)	2.52 (0.01)	2.50 (0.32)	2.51 (0.07)
S16	2.54 (0.02)	2.50 (0.14)	2.49 (0.00)	2.55 (0.00)	2.53 (0.11)	2.51 (0.09)	2.54 (0.16)
S17	2.58 (0.18)	2.51 (0.50)	2.53 (0.03)	2.57 (0.14)	2.55 (0.01)	2.55 (0.74)	2.55 (0.05)
S18	2.59 (0.59)	2.52 (0.76)	2.55 (0.82)	2.58 (0.49)	2.58 (0.51)	2.55 (0.10)	2.57 (0.73)
S19	2.61 (1.21)	2.53 (1.05)	2.56 (1.22)	2.59 (1.20)	2.60 (0.54)	2.57 (0.19)	2.58 (0.31)
S20	2.62 (1.49)	2.55 (0.86)	2.56 (1.38)	2.60 (1.00)	2.61 (1.55)	2.57 (1.21)	2.59 (1.09)
S21	2.67 (0.15)	2.56 (0.06)	2.57 (0.05)	2.61 (0.32)	2.62 (0.59)	2.58 (0.91)	2.60 (0.19)
S22	2.67 (0.04)	2.59 (0.30)	2.58 (0.04)	2.63 (0.18)	2.63 (0.40)	2.58 (0.55)	2.62 (0.71)
S23	2.69 (0.22)	2.60 (0.16)	2.60 (0.40)	2.64 (0.01)	2.65 (0.14)	2.61 (0.01)	2.62 (0.87)
S24	2.70 (0.15)	2.65 (0.01)	2.62 (0.07)	2.65 (0.38)	2.66 (0.01)	2.64 (0.03)	2.63 (0.08)
S25	2.74 (0.06)	2.67 (0.05)	2.66 (0.05)	2.69 (0.06)	2.68 (0.15)	2.69 (0.00)	2.68 (0.01)

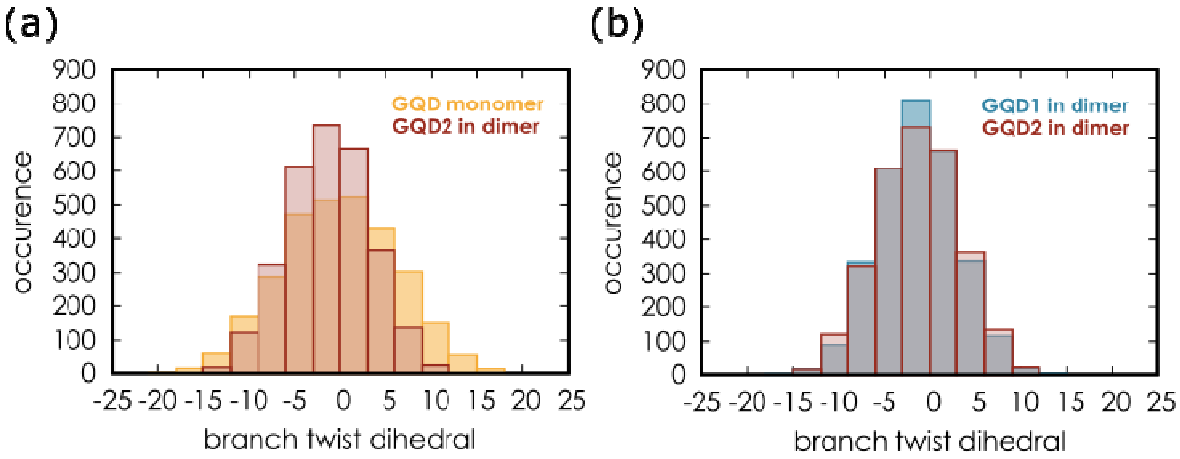

Figure S4. Out-of-plane distortion within $C_{96}C_{12}$ GQD: distributions of the branch twist dihedral angle (°) of the GQD branches with respect to the median plane: (a) monomer (yellow) and GQD2 in the dimer (red). (b) GQD1 (blue) and GQD2 (red) in the dimer.

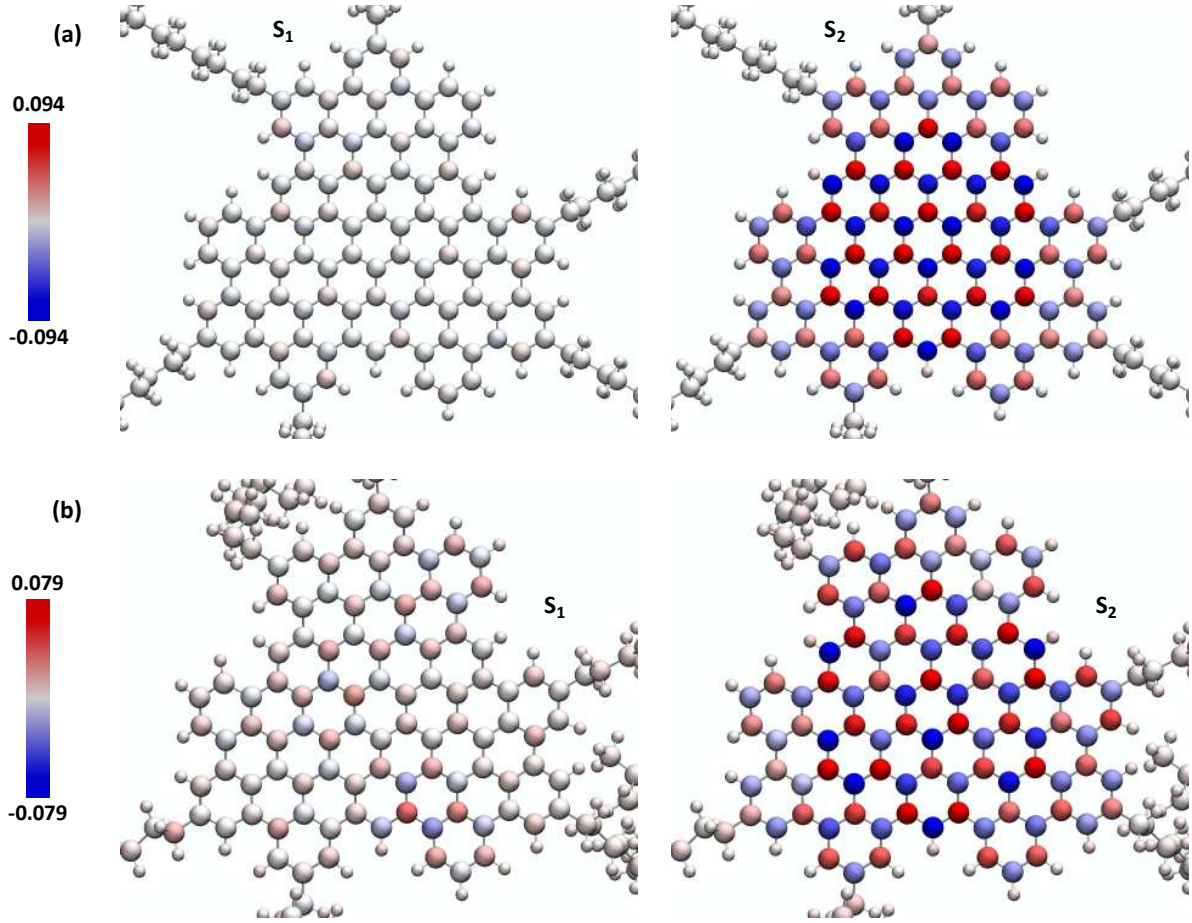

Figure S5. Transition ESP charges for the $S_0 \rightarrow S_1$ and $S_0 \rightarrow S_2$ transitions computed at (a) the ground state geometry and (b) distorted geometry extracted from MD (frame b975 in table S4).

Absorption and PL spectra of two suspensions from the same batch

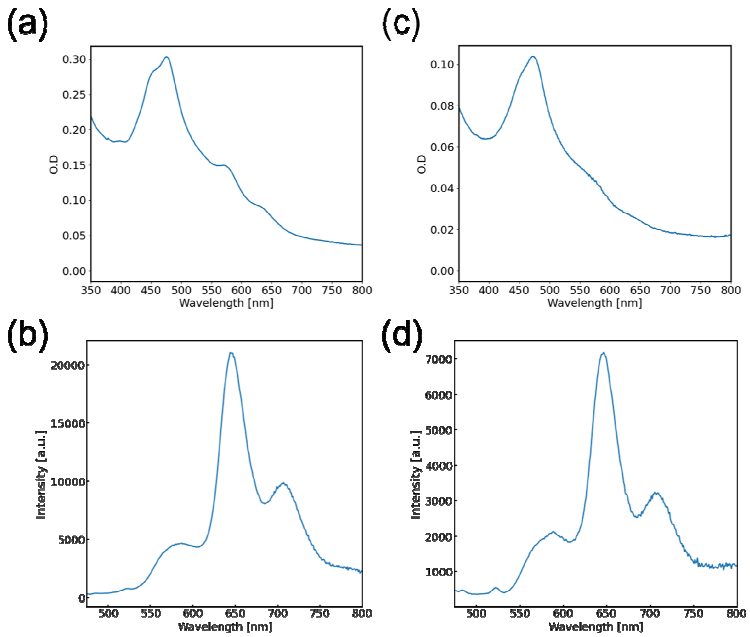

Figure S6. (a) & (c) Absorption spectra, (b) & (d) PL spectra of two suspensions of $C_{96}C_{12}$ of the same batch in TCB.

The figure S6 (a) and (c) shows two absorption spectra of two suspensions of $C_{96}C_{12}$ in TCB obtained from the same batch (same synthesis). One can see that the main features are of course preserved. Nevertheless, some differences are also observed. The main one concerns the structuration of the absorption lines. On the left spectrum, the absorption main line shows distinct structures at ~450 nm and 480 nm. Likewise, two structures are also observed at ~580 nm and ~640 nm. On the spectrum depicted on the right-hand side of the figure, all these structures are much less pronounced. This may be related to a different degree of aggregation in the suspension. Likewise, figure S6 (b) and (d) display the corresponding PL spectra recorded in the same experimental conditions. The intensities can therefore be compared. First the intensity of line 1 normalized by the optical density at 480nm is almost the same in both samples. On the contrary, the line 1 over line 3 intensities ratio is ~4.3 in figure S6(b) while it's 3.5 in figure S6(d). This rules out the possibility that line 3 originates only from impurities.

Absorption spectra of the different batches of $C_{96}C_{12}$ and corresponding time evolution of the PL spectra

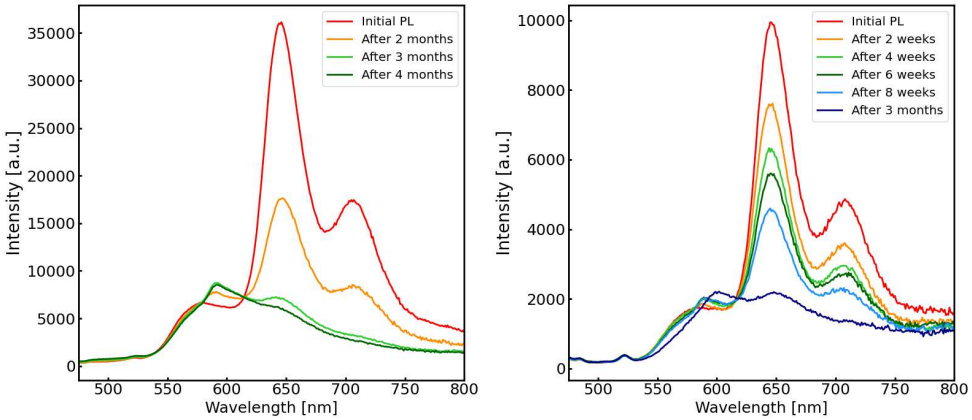

Figure S7. Time evolution of two other suspensions of $C_{96}C_{12}$ in TCB.

Detailed analysis of the MALDI-TOF Spectrum

The main peak at m/z~2191 is attributed to the $C_{96}C_{12}$ structure. Below this peak, nothing is detected in the MALDI-TOF spectra. At higher *m/z* ratio than the molecular ion peak some small peaks can be observed certainly related to remaining synthesis by-products. There is no uniqueness in the allocation of these lines. The peak at ~Δ *m/z* = 12 can be related to a non-closed product (see Figure S10). Likewise, the structure at ~Δ *m/z* = 34 can be related to the $C_{96}C_{12}$ GQD with one chlorine atom. The next peaks pattern is located at ~Δ *m/z* = 76, whom attribution is more challenging. $C_{96}C_{12}$ GQD with 2 or 3 chlorine atoms lead to exact mass of 2259.3 and 2293.2, not compatible with this ~Δ *m/z* = 76 peaks pattern. Potential possibilities for these peaks include a complex with a Fe atom accompanied by an OH group (see Figure S11), with some bonds missing. The two next peaks at ~Δ *m/z* = 110 and ~Δ *m/z* = 144 may correspond to the substitution of hydrogen atoms with chlorine (Δ *m/z* = 34) to the previous structures. The simulated mass spectra were performed using Free-to-use Prot pi Mass Spec Simulator (https://www.protpi.ch/Calculator/MassSpecSimulator).

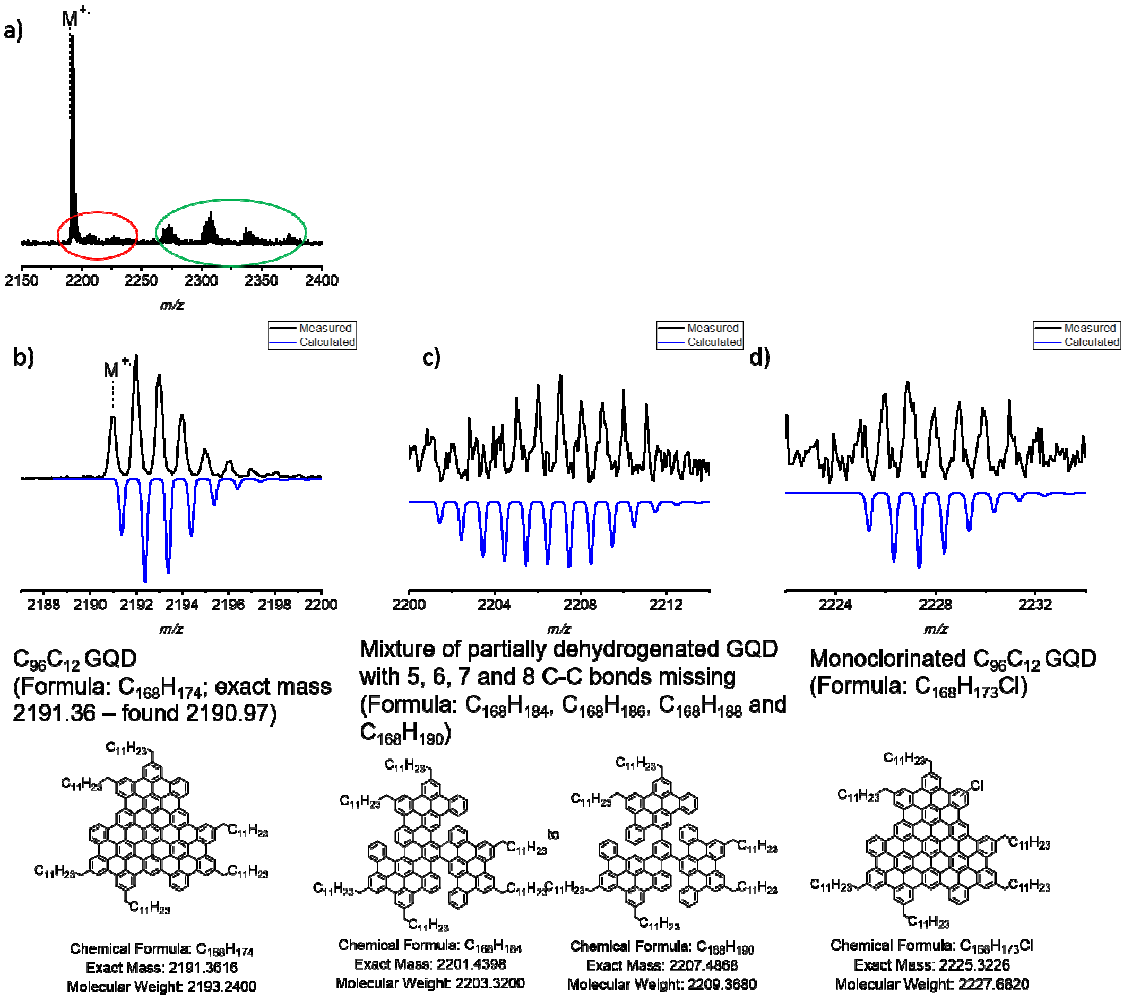

Figure S9: MALDI-TOF spectrum of the $C_{96}C_{12}$ batch used in this study. a), b), c) Zoom on specific mass region circled in red and possible structure assignations. a) Molecular ion peaks in black and simulated spectrum in blue; b) in the *m/z* = 2000-2212 region, the peaks can be attributed to partially dehydrogenated GQD, the simulation shows that 5 to 8 C-C bonds are missing; c) in the *m/z* = 2224-2232 region, the peaks are attributed to the mono-chlorinated $C_{96}C_{12}$ GQD (chlorination is often observed during Scholl reaction using $FeCl_3$). The peaks in the green circle region are discussed in Figure S11.

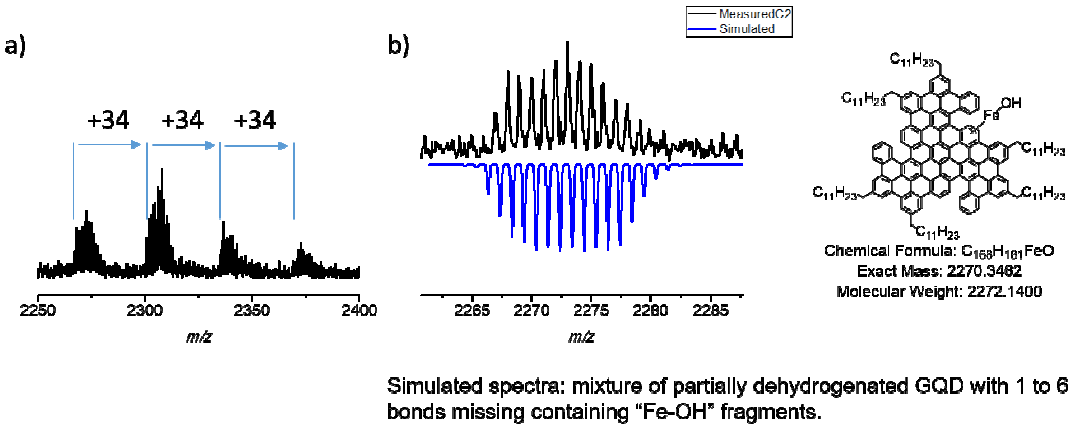

Figure S10. MALDI-TOF spectrum of the $C_{96}C_{12}$ batch used in this study (green circle region of Figure S10). The peaks do not correspond to multiple addition of chlorine atoms on the $C_{96}C_{12}$ GQD structure but may correspond to salts including partially dehydrogenated GQD. These structures are highly speculative and no spectral or isotopic pattern can be extracted from the measured spectra.

Transmission electron microscopy

Transmission electron microscopy (TEM) imaging was done using monochromated and aberration corrected TEM (Thermo Fisher, Titan Ultimate) performing at 80~kV. The GQD samples were dispersed on a monolayer CVD graphene (Graphenea) pre-deposited on C-flat TEM grid. The signal of graphene support layer was removed during the data treatment using low-pass filter on the Fourier transform of each image.

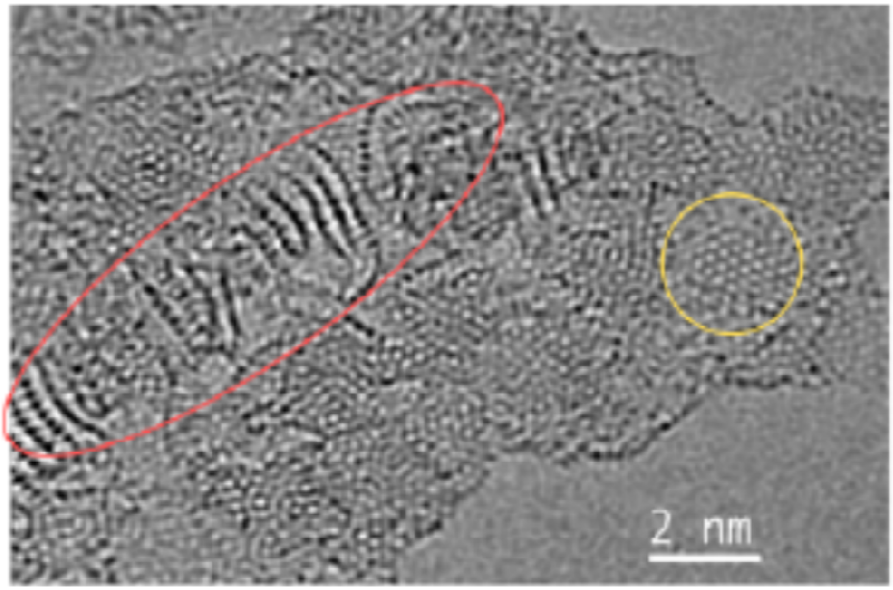

Figure S11. TEM images of the GQDs solution deposited on a monolayer CVD graphene (Graphenea) pre-deposited on C-at TEM grid. Both small particles corresponding to monomer GQD or small aggregate (yellow circle) and columnar structures made of stacked GQDs (red circle) are observed. Here the column lays on its side.